

Three-Dimensional Superconductivity in the Infinite-Layer Compound $\text{Sr}_{0.9}\text{La}_{0.1}\text{CuO}_2$ in Entire Region below T_c

Mun-Seog Kim, C. U. Jung, J. Y. Kim, Jae-Hyuk Choi, and Sung-Ik Lee

National Creative Research Initiative Center for Superconductivity and Department of Physics, Pohang University of Science and Technology, Pohang 790-784, Republic of Korea

(October 31, 2018)

The infinite-layer compound ACuO_2 ($A =$ alkaline-earth ions) is regarded as the most suitable material for exploring the fundamental nature of the CuO_2 plane because it does not contain a charge-reservoir block, such as a rock-salt or a fluorite like block. We report that superconductivity in the infinite-layer compound $\text{Sr}_{0.9}\text{La}_{0.1}\text{CuO}_2$ is of a three-dimensional nature, in contrast to the quasi two-dimensional superconducting behavior of all other cuprates. The key observation is that the c -axis coherence length is longer than the c -axis lattice constant even at zero temperature. This means that the superconducting order parameter of one CuO_2 plane overlaps with those of neighboring CuO_2 planes all the temperatures below the T_c . Among all cuprates, only the infinite-layer superconductor shows such a feature.

The key ingredient of high-temperature superconductors (HTSC) is the CuO_2 plane in which superconductivity occurs. Besides the CuO_2 plane, the unit cell of HTSC generally contains a charge-reservoir block (CRB) which supplies holes or electrons into the conducting layer. However, the function of the CRB, beyond supplying carriers in the materials, is not yet completely clear. In one respect, the CRB might simply be a spacer between the CuO_2 planes. In this case, the block reduces the layer-by-layer coupling. The strong anisotropic nature of HTSC is believed to be a reflection of this weak interlayer coupling. In this context, the infinite-layer compounds ACuO_2 ($A =$ alkaline-earth ions) are remarkable, because they do not have a CRB, so the simplicity of their crystal structure may allow in-depth insight into the basic mechanism of cuprate superconductivity. Due to the absence of the CRB, infinite-layer compounds have two notable features. First, the distance from one unit cell to the next is the *shortest* among all the cuprates. [1] Secondly, as a matter of course, charge carriers can be supplied only from the cations at the A sites. For example, the carrier density of the stoichiometric infinite-layer SrCuO_2 is zero. The partial substitution of La^{+3} (or Nd^{+3}) for Sr^{+2} results in superconductivity in these compounds. [2] In this case, the carriers are not holes, but electrons. [3–6]

Recently, we successfully synthesized pure-phase $\text{Sr}_{0.9}\text{La}_{0.1}\text{CuO}_2$ (Sr(La)-112) with $T_c \simeq 43$ K by using a cubic multi-anvil press. The details of the sample preparation will be given elsewhere. [7] In this work, we measured the reversible magnetization as a function of the temperature and the angle between the c axis and the applied magnetic field. From analysis of the data, we found that the usual HTSC two-dimensional (2D) temperature region of $\xi_c(T) < c$ below T_c did not exist in this compound. This peculiar feature has not been observed

in any other high- T_c material. Until now, $\text{YBa}_2\text{Cu}_3\text{O}_{7-\delta}$ (Y-123) has been known to have the most strong inter-layer coupling, but the three-dimensional (3D) temperature region is limited to near T_c only. Previously, [8] it was claimed that the high- T_c superconductivity occurred only on the 2D network of CuO_2 planes, since a 3D network did not permit spin or charge fluctuation while a 1D structure did not establish long range order of superconductivity. Hence, our observation of 3D superconductivity in entire region below T_c in Sr(La)-112 provides a new aspect of high-temperature superconductivity.

For the magnetization measurements, we aligned the grains of the sample in commercial epoxy under an external magnetic field of 11 T. [9–13] Fig. 1 displays the x-ray powder diffraction (XRD) pattern of Sr(La)-112 before and after the grain alignment. After the alignment, only the (002) reflection was seen in the XRD pattern. The inset of Fig. 1 shows the x-ray rocking curve of the (002) reflection. The full width at half maximum of the reflection is less than 1 degree, which means a good c -axis alignment. The aligned sample was approximately 9.5 mm in length and 3 mm in diameter. The reversible magnetization was measured as a function of the temperature and the angle between the c axis and the applied magnetic field by using a superconducting quantum interference device (SQUID) magnetometer (MPMS-XL, Quantum design).

Figure 2 shows the reversible magnetization, $4\pi M(T)$, at fields of $1 \text{ T} \leq H \leq 5 \text{ T}$ parallel to the c axis of the sample. In this figure, the symbols and the lines denote the zero-field-cooled and the field-cooled magnetizations, respectively. In comparison with other cuprates, our data show two interesting features. First, the curves shift to lower temperature as the field increases and are almost parallel to each other. This typical mean-field behavior is consistent with the prediction of the Abrikosov model

[14] in which the magnetization scales linearly with the magnetic field. Such a feature has never been observed before for any high- T_c cuprate because the mean-field behavior is usually screened by strong thermal fluctuations. [15] Secondly, the rate of decrease of $T_c(H)$ with respect to the field is significantly larger than that of other cuprates, here the superconducting transition temperature, $T_c(H)$, is estimated as the temperature at the point of intersection of a linear extrapolation of $4\pi M(T)$ in the superconducting state with the normal-state base line of $4\pi M = 0$. For instance, at $H = 5$ T, $T_c(H)$ is found to be about 33 K, which corresponds to $0.77T_c(0)$. Hence, the upper-critical field $H_{c2}(0)$ is expected to be about 20 T, assuming a linear $T_c(H)$. To determine $H_{c2}(0)$ precisely, we apply the Hao-Clem model for reversible magnetization [16,17] to our data. The details of the analysis will be given elsewhere (M.-S. Kim *et al.*, manuscript in preparation). Two important parameters characterizing the compound are the Ginzburg-Landau parameter, κ , and the slope of the upper-critical field near T_c , $dH_{c2}/dT|_{T_c}$. The Hao-Clem model analysis gives $\kappa = 25.3 \pm 1.1$ and $dH_{c2}/dT|_{T_c} = -0.47 \pm 0.02$ T/K. Using these, we estimate $H_{c2}(0)$ to be 13.9 ± 0.5 T through the relationship $H_{c2}(0) \simeq 0.7(dH_{c2}/dT)_{T_c}T_c$, [18] which is about ten times smaller than the value for other cuprate superconductors. The in-plane coherence length $\xi_{ab}(0) = [\phi_0/2\pi H_{c2}(0)]^{1/2}$ is calculated to be 48.6 ± 1.0 Å, where ϕ_0 is the flux quantum. [19]

In our study, we apply the Hao-Clem model to describe our magnetization data. [10–12] Since the model is derived from the phenomenological Ginzburg-Landau (GL) theory, our result is justified in the GL framework. However, we judge our result not to be model dependent particularly from the following consideration: The open symbols in the inset of Fig. 2 represent the in-plane magnetic penetration depth, $\lambda_{ab}(T)$, obtained from the dc-magnetic susceptibility, $4\pi\chi(T)$, for the low-field region of $H < H_{c1}$. To deduce $\lambda_{ab}(T)$ from the $4\pi\chi(T)$ curve, we use the Shoenberg formula, [20] which is not model dependent, but is merely based on the London equations. For comparison, we also plot $\lambda_{ab}(T)$ (filled symbols) from the Hao-Clem analysis in the same figure. We can see that the two curves, indeed, coincide. Thus, we can conclude that the application of the Hao-Clem model in this study does not reduce the generality of our results.

In the inset of Fig. 2, the solid line represents the temperature dependence of the penetration depth assuming the BCS clean limit. [14] The estimated zero-temperature penetration depth, $\lambda_{ab}(0)$, is 147 ± 6 nm, which is close to $\lambda_{ab}(0) \simeq 130$ nm of Y-123. In the framework of the London model, the penetration depth is proportional to $(m_{ab}^*/n_s)^{1/2}$, where m^* and n_s are the electronic effective mass in the ab plane and the charge-carrier density, respectively. According to the empirical Uemura relation, [21] *i.e.*, $T_c \sim n_s/m_{ab}^*$, the T_c 's of the two compounds

should be nearly the same. However, the T_c of Sr(La)-112 is about half that of Y-123. This discordance might differentiate Sr(La)-112 from the hole-doped cuprates.

For the cuprate superconductors studied until now, the zero-temperature coherence length along the c axis, $\xi_c(0)$, was found to be much smaller than the unit c -axis length. As the temperature increased toward T_c , a dimensional crossover from 2D to 3D occurred at a certain temperature T^* where $\xi_c(T^*) = c/\sqrt{2}$. [22] For moderately anisotropic materials like Y-123, a broader 3D-temperature region around T_c was observed due to strong interlayer coupling. [23] However, the 3D region for strongly anisotropic compounds, such as Bi- and Tl-based superconductors, was found to be extremely narrow. [24]

Since the unit structure of an infinite-layer superconductor does not contain a CRB, one can expect the coupling between CuO_2 planes to be strong. [25] To date, however, no rigorous studies to examine the dimensionality of the compound have been done. With our high-quality samples, we designed experiments to obtain the anisotropy ratio $\gamma = \xi_{ab}/\xi_c$. A combination of γ and the $\xi_{ab}(0)$ obtained above gives the ratio ξ_c/c which determines the dimensionality of the system.

Under an external magnetic field, the magnetization of all anisotropic materials has two components, M_L and M_T . M_L is the component parallel to the field, and the other component, M_T , is perpendicular to the field. Usually, M_T can be measured using a torque magnetometer, and the degree of anisotropy is reflected in the angular dependence of the torque, $\tau(\theta) = HM_T(\theta)$. Previously, Farrell *et al.* [26,27] measured the magnetic torque curves for highly anisotropic $\text{Bi}_2\text{Sr}_2\text{CaCu}_2\text{O}_8$ (Bi-2212) and moderately anisotropic Y-123. By applying the London model to the data, they obtained the anisotropy ratios $\gamma \simeq 55$ and $\gamma \simeq 5$ for Bi-2212 and Y-123, respectively. On the other hand, we obtained the anisotropy ratio of Sr(La)-112 by measuring $M_L(\theta)$ using a SQUID magnetometer with a sample rotator. The obtained data were analyzed by using the calculation of Hao *et al.* [16,17] which considered the effective mass anisotropy of the material. For comparison, we also applied the London model [14] to the data.

Figure 3 shows the angular dependence of the reversible magnetization, $4\pi M(\theta)$, measured at $H = 1$ T in the temperature range of $36.5 \text{ K} \leq T \leq 40 \text{ K}$. [28] In this figure, the solid lines represent the theoretical prediction of the Hao-Clem model. We see a good fit, except for temperatures above $T = 39$ K. We infer that the departure of the data from the theoretical lines at higher temperatures is due to the thermal fluctuation effect, which becomes more important as the temperature increases. [10,13] The inset of Fig. 3 is a plot of the anisotropy ratio obtained from each curve in Fig. 3. The filled and the open symbols are deduced by application of the Hao-Clem and the London models, respectively. In

the filled-symbol set, the curve shows a plateau behavior at low temperatures and then increases monotonically with temperature. The increase is postulated to originate from the thermal fluctuation effect, as mentioned above. In the open-symbol set, however, no such plateau feature exists. In fact, the London model is known to be suitable for the low-field region of $H \ll H_{c2}$. Since our magnetization data were taken near the transition temperature, the external field of 1 T is regarded as considerably large. Thus, our data set is out of the London region. This is consistent with the $4\pi M(T)$ data in Fig. 2, which lie in the Abrikosov region.

It is quite natural to take the value of the plateau in the filled-symbol set as the real anisotropy ratio. With this value, $\gamma = 9.3 \pm 0.2$, we obtain an out-of-plane coherence length of $\xi_c(0) = 5.2 \pm 0.3 \text{ \AA}$ by using the relationship $\xi_c = \xi_{ab}/\gamma$ and the value of $\xi_{ab}(0)$ from the above analysis. The criterion for 3D superconductivity below T_c is $\xi_c(T) > c/\sqrt{2}$. [22] The value of $\xi_{ab}(0) = 5.4 \text{ \AA}$ is considerably larger than the $c/\sqrt{2} \simeq 2.4 \text{ \AA}$. This means that the superconducting order parameter of one CuO_2 plane overlaps with those of neighboring CuO_2 planes even at zero temperature.

Additional evidence for 3D superconductivity can be found from the scaling analysis [10–13,24,29,30] of the fluctuation-induced magnetization for the high-field region. According to Ullah and Dorsey, [31] the magnetization in the critical region scales with the scaling variable of $A[T - T_c(H)]/(TH)^n$, where A is a field and transition temperature-independent coefficient, and n is 2/3 for a 3D system and 1/2 for a 2D system. As expected, the magnetization scales excellently with the 3D form. Figure 4 shows $4\pi M/(TH)^n$ versus the scaling parameter $(T - T_c(H))/(TH)^n$ with $n = 2/3$. All the data for the different fields collapse onto a single curve. The slope $-dH_{c2}/dT \simeq 0.5 \text{ T/K}$ near T_c is obtained from this scaling analysis. This value is fairly consistent with that deduced from the c -axis magnetization analysis.

Our results provide clear evidences for three-dimensional superconductivity, even at zero temperature, in the infinite-layer compound $\text{Sr}_{0.9}\text{La}_{0.1}\text{CuO}_2$. Here, we deduced the anisotropy ratio γ to be about 9 by measuring the angular dependence of the reversible magnetization. This value is somewhat larger than the value of $\gamma \simeq 5$ for Y-123. However, the absence of a CRB in the infinite-layer compound allows the order parameter of one layer to overlap with those of neighboring layers. In addition, we found that the empirical Uemura relation was not applicable to the case of $\text{Sr}_{0.9}\text{La}_{0.1}\text{CuO}_2$.

The authors thanks D. Pavuna, M. Sigrist, J. L. Tallon, P. Müller, and N.-C. Yeh for useful discussions. This work was supported by Creative Research Initiatives of the Korean Ministry of Science and Technology.

- [1] T. Siegrist, S. M. Zahurak, D. W. Murphy, and R. S. Roth, *Nature* **334**, 231 (1988).
- [2] M. G. Smith *et al.*, *Nature* **351**, 549 (1991).
- [3] J. D. Jorgensen *et al.*, *Phys. Rev. B* **47**, 14654 (1993).
- [4] G. Er, S. Kikkawa, M. Takahashi, and F. Kanamaru, *Physica C* **276**, 315 (1987).
- [5] E. C. Jones, D. P. Norton, D. K. Christen, and D. H. Lowndes, *Phys. Rev. Lett.* **73**, 166 (1994).
- [6] R.-S. Liu *et al.*, *Solid State Comm.* **118**, 367 (2001).
- [7] C. U. Jung *et al.*, *Physica C* (to be published).
- [8] K. Kitazawa, *Physica C* **341-348**, 19 (2000).
- [9] D. E. Farrell *et al.*, *Phys. Rev. B* **36**, 4025 (1987).
- [10] M.-S. Kim, C. U. Jung, S.-I. Lee, and A. Iyo, *Phys. Rev. B* **63**, 134513 (2001).
- [11] J.-H. Choi *et al.*, *Phys. Rev. B* **58**, 538 (1998).
- [12] M.-S. Kim *et al.*, *Phys. Rev. B* **57**, 8667 (1998).
- [13] M.-S. Kim *et al.*, *Phys. Rev. B* **57**, 6121 (1998).
- [14] M. Tinkham, *Introduction to Superconductivity*, 2nd ed. (McGraw-Hill, New York, 1996).
- [15] D. K. Finnemore, in *Phenomenology and Applications of High-Temperature Superconductors*, edited by K. S. Bedell *et al.* (Addison-Wesley, Massachusetts, 1992), p. 164.
- [16] Z. Hao and J. R. Clem, *Phys. Rev. Lett.* **67**, 2371 (1991).
- [17] Z. Hao *et al.*, *Phys. Rev. B* **43**, 2844 (1991).
- [18] N. R. Werthamer, E. Helfand, and P. C. Hohenberg, *Phys. Rev.* **147**, 295 (1966).
- [19] One of interesting points is that the superconducting parameters such as T_c , κ , $\xi_{ab}(0)$, $\lambda_{ab}(0)$, and the critical fields obtained in this study are the same as those of the newly discovered MgB_2 superconductor within 10% error range. (D. K. Finnemore *et al.*, *Phys. Rev. Lett.* **86**, 2420 (2001)).
- [20] D. Shoenberg, *Superconductivity* (Cambridge University, Cambridge, 1954).
- [21] Y. J. Uemura *et al.*, *Phys. Rev. Lett.* **66**, 2665 (1991).
- [22] D. E. Prober, M. R. Beasley, and R. E. Schwall, *Phys. Rev. B* **15**, 5245 (1977).
- [23] W. C. Lee, R. A. Klemm, and D. C. Johnston, *Phys. Rev. Lett.* **63**, 1012 (1989).
- [24] Q. Li, M. Suenaga, T. Hikata, and K. Sato, *Phys. Rev. B* **46**, 5857 (1992).
- [25] T. Imai, C. P. Slichter, J. L. Cobb, and J. T. Markert, *J. Phys. Chem. Solids* **56**, 1921 (1995).
- [26] D. E. Farrell *et al.*, *Phys. Rev. Lett.* **63**, 782 (1989).
- [27] D. E. Farrell *et al.*, *Phys. Rev. Lett.* **61**, 2805 (1988).
- [28] Below $T \simeq 36 \text{ K}$, the angular dependence of magnetization is severely asymmetric with respect to the angle $\theta = \pi/2$, which means that the sample does not enter an reversible state for entire region of θ , *i.e.*, $0 \leq \theta \leq \pi$.
- [29] Z. Tešanović *et al.*, *Phys. Rev. Lett.* **69**, 3563 (1992).
- [30] J. Sok *et al.*, *Phys. Rev. B* **51**, 6035 (1995).
- [31] S. Ullah and A. T. Dorsey, *Phys. Rev. Lett.* **65**, 2066 (1990).

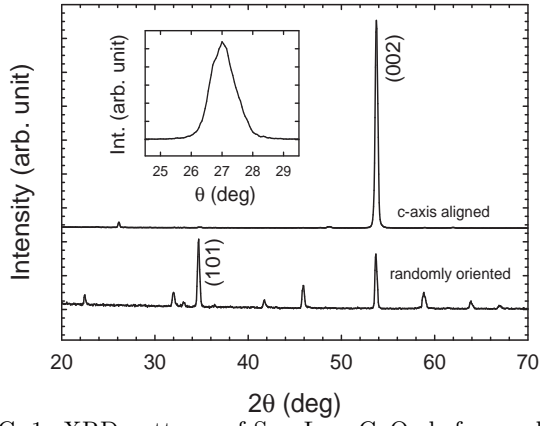


FIG. 1. XRD patterns of $\text{Sr}_{0.9}\text{La}_{0.1}\text{CuO}_2$ before and after the grain alignment. The inset shows x-ray rocking curve of the (002) reflection of aligned sample.

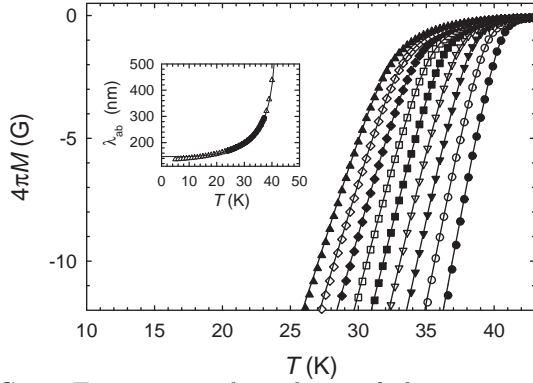


FIG. 2. Temperature dependence of the magnetization, $4\pi M(T)$, measured at applied magnetic fields of $1 \text{ T} \leq H \leq 5 \text{ T}$ (filled circles, 1 T; open circles, 1.5 T; filled down triangles, 2 T; open down triangles, 2.5 T; filled squares, 3 T; open squares, 3.5 T; filled diamonds, 4 T; open diamonds, 4.5 T; filled up triangles, 5 T). The inset shows the penetration depth, $\lambda_{ab}(T)$, deduced from the Hao-Clem model (filled symbols) and the Shoenberg formula (open symbols). In this figure, the solid line represents the BCS temperature dependence of the penetration depth.

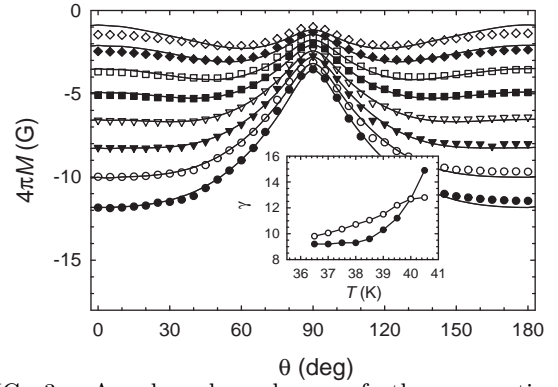


FIG. 3. Angular dependence of the magnetization, $4\pi M(\theta)$, measured at temperatures of $36.5 \text{ K} \leq T \leq 40 \text{ K}$ and a field of $H = 1 \text{ T}$ (filled circles, 36.5 K; open circles, 37 K; filled down triangles, 37.5 K; open down triangles, 38 K; filled squares, 38.5 K; open squares, 39 K; filled diamonds, 39.5 K; open diamonds, 40 K). The θ denotes the angle between the applied magnetic field and the crystallographic c axis of the sample. The solid lines represent the prediction of the Hao-Clem model. The inset shows the anisotropy ratio $\gamma(T)$ obtained from $4\pi M(\theta)$. The filled and the open symbols are deduced from analyses based on the Hao-Clem and the London models, respectively. The solid lines are just guides for the eyes.

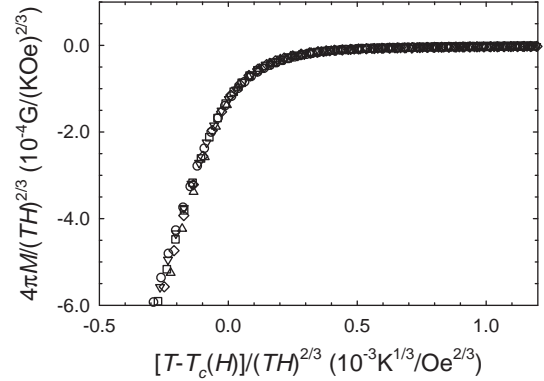


FIG. 4. Scaling of the data of Fig. 1 with the scaling variable $(T - T_c(H)) / (TH)^{2/3}$. In this analysis, a linear temperature dependence of H_{c2} near T_c was used assumed, *i.e.*, $-dH_{c2}/dT = 0.47 \text{ T/K}$.